Colloids and Surfaces A: Physicochemical and Engineering Aspects 633 (2022) 127874

Contents lists available at ScienceDirect

Colloids and Surfaces A: Physicochemical and Engineering Aspects

journal homepage: www.elsevier.com/locate/colsurfa

Oil soluble surfactants as efficient foam stabilizers

Fatmegyul Mustan [a], Nadya Politova-Brinkova [a], Damiano Rossetti [b], Pip Rayment [b], Slavka Tcholakova [a,*]

[a] Department of Chemical and Pharmaceutical Engineering Faculty of Chemistry and Pharmacy,University of Sofia, 1 James Bourchier Ave., 1164 Sofia, Bulgaria
[b] Unilever R & D, Colworth, UK

HIGHLIGHTS

- Hydrophobic surfactants (Span 60 and Brij 72) form foams with small bubbles.
- The stability of Span 60 foams is higher as compared to Brij 72 foams.
- The higher stability is related to higher viscosity and high surface stress.
- Surface tensions of shrinking and expanding bubbles are very different.
- This difference decreases the driving force for Ostwald ripening.

GRAPHICAL ABSTRACT

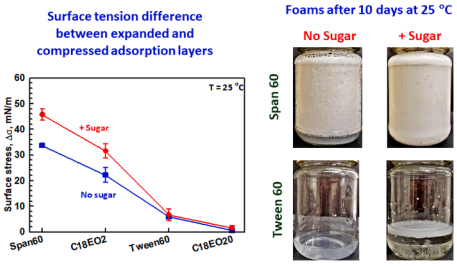

ARTICLE INFO

Keywords:
Sugar
Tween 60
Span 60
Brij 72
Brij S20
Surface properties
Foam stability
Foam rheology

ABSTRACT

The surface and foam properties of two oil-soluble surfactants, Span 60 and Brij 72, and two water-soluble surfactants, Tween 60 and Brij S20, are compared. Aqueous surfactant solutions containing sugar at high concentration (63 wt%) are also studied in the context of sweet food-related foams. The experimental results show that foams with very small bubbles of ca. 5 μm are formed and remain stable for more than 10 days at room temperature when oil-soluble surfactants are dispersed in the sugar-rich solutions. The excellent stability of these foams is related to (1) The multilamellar vesicles present in the respective surfactant dispersions which increase the viscosity and decrease the rate of water drainage from the foam; (2) The very slow exchange of surfactant molecules between the interface and the adjacent aqueous solution that leads to very significant difference in the surface tension of shrinking and expanding bubbles, which in turn decreases the rate of bubble Ostwald ripening. The foams formed from Span 60 are more stable as compared to the foams formed from Brij 72, due to the higher viscosity and the slower interface-solution exchange. The foams formed from Brij S20 solutions are least stable - they are completely destroyed after 1 day at room temperature, even in the presence of sugar. The main conclusion of this study is that oil soluble surfactants can form condense adsorption layers on the bubble surfaces after adsorption from aqueous solutions with and without sugar in it. The formed layers, which present a better molecular packing, reduce the gas permeability and decelerate the Ostwald ripening disproportionation of the foam This is obtained by a relatively low interfacial tension imparted by continuous shrinkage and expansion of bubbles during foam generation, ultimately ensuring long-term stabilization of formed foams.

* Correspondence to: Department of Chemical and Pharmaceutical Engineering, Faculty of Chemistry and Pharmacy, Sofia University, 1 James Bourchier Ave., 1164 Sofia, Bulgaria.
E-mail address: sc@lcpe.uni-sofia.bg (S. Tcholakova).

https://doi.org/10.1016/j.colsurfa.2021.127874
Received 29 August 2021; Received in revised form 1 November 2021; Accepted 5 November 2021
Available online 17 November 2021

1. Introduction

Bulk, surface and foaming properties of nonionic surfactants are widely studied in the literature due to their importance for various industries [1–6]. Water-soluble surfactants are usually used for foam stabilization [7–11], whereas oil-soluble surfactants are used for stabilization and destabilization of emulsions [6,12–13] or as co-surfactants for foam stabilization [14,15]. It was shown that the usage of oil-soluble Spans 20, 80 and 85 leads to lower foamability and lower stability of formed foams as compared to foams formed from water-soluble surfactants [9]. On the other hand, Chen et al. [7] showed that stable foams can be formed from 10 wt% dispersion of oil soluble surfactant $C_{12}EO_3$, but at lower concentration of 1 wt% there is almost no foam at all. The stability of foams formed from 30 wt% $C_{12}EO_3$ and $C_{12}EO_5$ was higher as compared to stability of foams formed from $C_{12}EO_7$ and $C_{12}EO_9$ solutions at the same surfactant concentration and this effect was explained with adsorption of lamellar liquid crystalline phases at air-water interface and their presence in the continuous phase, which increases the viscosity of the dispersion and decelerate the rate of water drainage [7].

In our previous studies [15–17] we showed that the rate of Ostwald ripening can decrease significantly upon formation of condensed adsorption layers on the bubble surfaces, due to high resistance to gas transfer of these layers. It is known from the literature that oil soluble surfactants such as Span 60, $C_{16}EO_1$, $C_{16}EO_2$ and $C_{18}EO_1$ are able to form condense adsorption layers upon compression in Langmuir trough [18–21], which means that these layers could decrease the rate of gas transfer if used them as foam stabilizers. However, it is very difficult to stabilize the bubbles by using oil soluble surfactants due to their low solubility in water and slow adsorption on the air-water interface. One possible way to overcome this problem is to use the knowledge from our recent studies [10,11], where is shown that the foamability depends not only on the rate of surfactant adsorption but also on the method that is used for foam generation. In Ref. [11] is shown that long chain nonionic surfactants such as Tween 60 and Brij58 are unable to stabilize the voluminous foam using fast foaming method (Barstch test), but they are very suitable to stabilize the foam formed in Kenwood mixer [11]. That is why in the current study Kenwood mixer is used to prepare the foams in presence of oil soluble surfactants alone and to compare their properties with foams stabilized by water soluble surfactants, Tween 60 and Brij S20.

The rate of Ostwald ripening depends also on the rate of gas diffusion through the continuous phase, which in turn depends on continuous phase viscosity [16,17]. One way to increase the viscosity of the continuous phase is to add sugar to it. Sugar is a main component in most sweet foods, such as milkshakes, cakes, candies, ice cream, etc. and it is added not only as a sweetener but also as ingredient which affects the mouthfeel and the texture of the products and it affects also the surface properties of oil-soluble surfactants such as monostearin and monopalmitin [22–25]. It was shown also that the presence of sugar in the protein solutions can affect their foamability [22-24] and the stability of formed foams [26,27]. Dressaire et al. [28] showed that the mixture of sucrose stearate and highly viscous glucose syrup (75 wt%) could produce aerated liquids with bubble size of 1.5 μm and air volume fraction of 45% which remained stable at 4 °C for more than 1 year. The extremely high stability of the produced aerated liquid was attributed to the formation of an elastic, condensed surfactant phase on the bubble surface which prevented the bubble disproportionation. Very good stability of foams upon storage is determined for foams stabilized by solid particles [16–17, 29], hydrophobin [30,31], saponins [16,32], surfactants forming lamellar phases in the bulk [33]. Oil-soluble surfactants formed multilamellar vesicles in the solutions and can be considered as soft particles, but they could be even more efficient as compared to solid particles, because the amount of surfactant that is required to cover the bubble surface will be much smaller as compared to particles if dense adsorption layer could be formed on the bubble surface.

In the current study we investigated: (1) Foamability; (2) Bubble size; (3) Foam stability against drainage, coalescence and Ostwald ripening and (4) Rheology of foams formed from dispersions of two oil-soluble surfactants, Span 60 and Brij 72, and two water-soluble surfactants, Tween 60 and Brij S20 without and with (63 wt%) sugar in the solution. The surface properties of the surfactant solutions were characterized by several experimental methods to determine the surface elasticity and viscosity under slow and fast surface deformations. The bulk solution properties were characterized with respect to their viscosity, the presence of micelles or multi-lamellar vesicles, MLV, and the phase transition temperature of the surfactant aggregates is measured by DSC.

2. Materials and Methods

2.1. Materials

Two of the studied surfactants are oil-soluble: Span 60 (Sorbitan stearate, product of Croda) and Brij 72 (Polyoxyethylene (2) stearyl ether, product of Sigma Aldrich denoted as $C_{18}EO_2$ in the text). The other two surfactants are water-soluble: Tween 60 (Polyethylene glycol sorbitan stearate, product of Croda) and Brij S20 (Polyoxyethylene (20) stearyl ether, product of Sigma Aldrich denoted as $C_{18}EO_{20}$ in the text). All surfactants were used without further purification. Sucrose, kindly donated by Unilever, was used as received. The solutions for the experiments were prepared with deionized water obtained by Elix 3 system (Merck-Millipore Inc., USA).

The studied solutions were prepared using the following procedure: (1) Deionized water or deionized water containing 64.3 wt% sugar was heated up to 75 °C in water bath. (2) Surfactant was added to the preheated solution and was homogenized with Ultra Turrax (Janke & Kunkel GmbH & Co, IKA-Labortechnik) for 5 min at 8 000 rpm keeping the temperature at 75 °C by water bath. (3) The prepared solution was cooled down to 25 °C in a cold-water bath with temperature of 10 °C. After reaching the temperature of 25 °C, the obtained surfactant solution was used for further experiments. The final concentrations of the substances in all solutions were: 2 wt% surfactant, with or without 63 wt% sucrose.

2.2. Methods

2.2.1. Optical observations in polarized light

Samples from the surfactant solutions were transferred onto microscope glass slides and were observed by optical microscope Axio Imager M2m (Zeiss, Germany) in transmitted, cross-polarized white light using long-focus objectives × 20, × 50 or × 100. The polarizer and analyzer were oriented at 90° with respect to each other. An additional λ plate (compensator plate) which was integrated in the analyzer was used to increase the contrast; it gave the typical magenta color for the liquid background.

2.2.2. Differential scanning calorimetry (DSC) analysis

Samples from the solutions were analyzed using Perkin-Elmer DSC7 apparatus for determination of the phase transition temperature. All sucrose containing solutions were heated from 20 °C to 80 °C and then cooled down back to 20 °C. The solutions without sucrose were heated from 20 °C to 68 °C (instead of 80 °C) due to the significant water evaporation at temperatures above 70 °C and then cooled down to 20 °C. The obtained thermograms upon cooling are presented and discussed below. All experiments were performed at 5 °C/min rate of heating/cooling.

2.2.3. Viscosity measurements

The viscosity of the solutions was measured on Discovery HR-3, TA Instruments USA, equipped with cone and plate geometry with diameter of 40 mm, cone angle of 1.007°, and truncation gap of 28 μm. The shear

rate was varied logarithmically and stepwise from 0.1 s^{-1} to 1000 s^{-1}. All samples were left for 2 min prior their measurement to equilibrate at 20 °C.

2.2.4. Surface tension measurements

Axisymmetric drop shape analysis (DSA) of a pendant drop was used to determine the equilibrium surface tension. The experiments were performed on instrument DSA100R and the profile of the drop was fitted by software DSA1, Krüss GmbH, Germany, to determine the surface tension. These experiments were performed at 25 °C and at least three measurements for each solution were made – the mean values with their standard deviations are presented in the text.

2.2.5. Characterization of surface rheological properties of adsorption layers

To characterize the rheological properties of the adsorption layers, the experiments under slow and fast deformations are performed. Oscillating drop method (ODM) on DSA 100 automated instrument to apply fast sinusoidal deformation on a pendant drop deformed by gravity is used for experiments under fast deformation. The oscillatory deformation was applied 10 min after the drop formation with amplitude of deformation between 6% and 10% and period of oscillations between 2 and 10 s. For each solution, at least 3 measurements were performed and the mean values and standard deviations are presented in the text.

Langmuir trough (Nima Technology Ltd., U.K.) is used to measure the change of surface tension due to adsorption of surfactant from solution to the interface. It was used to apply slow and large deformations on a planar surface. The area of the trough was varied with two parallel barriers that moved symmetrically at defined linear speed. The surface pressure was measured with Wilhelmy plate made of chromatographic paper. The plate was positioned in the middle between the barriers and was oriented parallel to them. Slow compressions reaching 107% (from 200 cm^2 to 68 cm^2) of surface deformation and following expansions were applied at barrier speed corresponding to area variation of 5 cm^2/min. In this experiment the time required to reach 10% deformation is 240 s, whereas in fast oscillation experiments it is 10 s, which shows that in Langmuir trough the deformations are performed at 24-times slower deformation rate as compared to the oscillations in ODM. After each deformation, a period of surface relaxation was monitored at fixed surface area for 30 min after compression and for 10 min after expansion. All measurements were performed at 25 °C. The deformation given in the text is the absolute value of deformation defined as $\alpha[\%] = 100|\ln A(t)/A_0|$, where $A(t)$ is the surface area after time t and A_0 is the initial surface area [34].

2.2.6. Foam generation

Foams were generated by mixing 230 ml of the solution for 1 h in Kenwood kMix food mixer equipped with whisk accessory at speed mark 5 (~ 425 rpm) and temperature of 25 °C, which was maintained by jacketed bowl. The mixing tool rotates around two axes - the first one is the axis of the mixing tool, whereas the second one is in the center of the vessel which contains the foamed solution. Detailed information about the hydrodynamic conditions in this device can be found in our previous study [31]. In Ref. [11] it was shown that the characteristic time for creation of new bubble surfaces is of around 15 s. In the current study, much longer time for mixing was applied in order to ensure enough time for oil-soluble surfactants to adsorb on bubble surface and to create dense adsorption layer.

2.2.7. Bubble size measurements

The bubble size distribution in the foam prepared from surfactant solutions without added sucrose was determined using the procedure developed by Garrett et al. [15,36]. A video camera, equipped with long-working-distance magnifying lens, was focused on a certain region in the foam sample, which was in contact with a glass prism, and used to capture images of the bubbles. The bubble size distribution was determined from these images using the relation $R_B = (A_{BP}/\pi)^{1/2}$, where A_{BP} is the projected area of a given bubble in contact with the prism wall. Image analysis software was used to determine the distribution of the projected bubble areas on the prism wall after 1, 3, 5, 7, 10, 30 and 60 min of foaming.

The bubble sizes of the foams containing 63 wt% of sucrose after 1, 3, 5, 7, 10, 30 and 60 min of foaming were measured by direct optical observations of the produced foams. For this purpose, samples were transferred onto microscope glass slides in a foam layer of 0.17 mm thickness and observed by optical microscope Axio Imager M2m (Zeiss, Germany) in transmitted light using long-focus objectives × 20 or × 50. The diameters of the recorded bubbles were measured by experienced operator, with custom-made image analysis software. Each bubble was measured individually. For each sample, the diameters of at least 1000 bubbles were measured. The mean volume-surface diameter, d_{32}, was determined:

$$d_{32} = \left(\sum_i N_i d_i^3\right) \Big/ \left(\sum_i N_i d_i^2\right) \quad (1)$$

where N_i is the number of bubbles with diameter d_i. As a characteristic of foam polydispersity, the ratio d_{32}/d_{10}, viz. the ratio between the mean volume-surface diameter and the mean arithmetic diameter of the bubbles was used.

2.2.8. Rheological properties of the foams

The rheological properties of the prepared foams after 60 min of foaming were characterized by rotational rheometer (Bohlin Geminin, Malvern UK). All measurements were made using two parallel plates with radius of 40 mm and gap between them set at 1 mm for sucrose containing foams and 2 mm for those without sucrose. Sandpaper of type P2000 or P150 was glued on both plates to eliminate the possible foam-wall slip. Tests in oscillatory and steady deformations were performed using the following protocols: (1) Strain-controlled frequency sweep – the frequency was logarithmically varied from 0.01 to 20 Hz. The strain was fixed at 1%. The elastic and viscous moduli of the samples were determined. (2) Frequency-controlled amplitude sweep – the strain was logarithmically varied from 0.01% to 100%. The frequency was fixed at 1 Hz. The elastic and viscous moduli of the samples were determined. (3) Shear ramp – the shear rate was varied logarithmically and stepwise from 0.1 to 200 s^{-1}. The shear stress, τ, was monitored as a function of the shear rate. All measurements were made at 25 °C.

The most of the experiments are performed in triplicate and mean value and standard deviation are reported in the manuscript.

3. Results and Discussions

3.1. Bulk properties

The surfactant solutions were transparent when water-soluble surfactants (Tween 60 and $C_{18}EO_{20}$) were dispersed in deionized water or in sugar solution. In contrast, the dispersions of oil-soluble surfactants (Span 60 and $C_{18}EO_2$) were turbid with and without sucrose in the aqueous phase. However, the addition of sucrose strongly affected the stability to sedimentation of the dispersions obtained with oil-soluble surfactants. These dispersions were unstable in deionized water while they remained stable in sucrose solutions. The instability of Span 60 solution in deionized water led to the formation of sediment at the bottom of the container, whereas a cream was formed for $C_{18}EO_2$ on top of the solution.

To determine the type of surfactant aggregates formed in these solutions the optical observations in polarized light were performed. No any entities were visible in Tween 60 and $C_{18}EO_{20}$ solutions with and without sugar, see Fig. S1in Supporting information, which indicated that these were micellar solutions with nanometer sized aggregates,

which is in good agreement with results available in the literature [37–40]. In contrast, micrometer sized spheroidal multi-lamellar vesicles, MLV were observed in Span 60 and $C_{18}EO_2$ dispersions, see Fig. 1. They are formed upon increase of temperature up to 75 °C and shearing of the dispersion [41–43]. The aggregates observed in Span 60 dispersion in deionized water were no clear colors in polarized light. In presence of sucrose, round aggregates of Span 60 with the characteristic Maltese crosses were observed which indicated the formation of multi-lamellar vesicles of onion structure [41–43]. Interestingly, such multi-lamellar onion mesophases were observed in $C_{18}EO_2$ dispersions in water with and without sugar added.

To determine the temperature at which the transition from L_α (melted chains) to L_β (frozen chains) [44,45] occurs in the aggregates of oil-soluble surfactants DSC measurements are performed, see Fig. 2. For water-soluble surfactants there are not detectable peaks in the thermogram, because the surfactants in the micelles did not undergo any phase transition in the temperature range studied. For oil-soluble surfactants the transition temperatures were ≈ 50.1 ± 0.5 °C for $C_{18}EO_2$ in water and ≈ 48.3 ± 0.3 °C in sucrose solution, whereas for Span 60 the transition temperature was 52.9 °C in water and 53.5 °C in sucrose solution, see Table S1 in Supporting information. The latter temperature is in a reasonable agreement with the available data for the phase transition of 20 wt% Span 60 in water, ≈ 55.2 ± 0.6 °C [46]. For both studied oil-soluble surfactants there was a significant increase in the enthalpy of the transition in the presence of sucrose which shows that sucrose enhances the molecular packing in the multi-lamellar vesicles [44]. Note that the ordered structures consume more energy for melting upon heating when compared to the disordered ones.

The results about the viscosity of the dispersions are shown in Fig. 3. For water-soluble surfactants the rheological response was Newtonian and the relative viscosity of the water soluble surfactant solutions with sucrose was by approx. 2 times higher than that without added sucrose. The latter comparison shows that the sucrose affects in some extent the size, shape or the interactions of the surfactant micelles. To check for the effect of sucrose on size of Tween 60 micelles DLS measurements were performed and it was found that the mean volume diameter increases from 9.5 ± 0.5 nm (without sucrose) to 37.3 ± 1.3 nm in presence of sucrose. Larger in size micelles in sucrose is probably the reason for 2-times increase in the relative viscosity when sucrose solution is used.

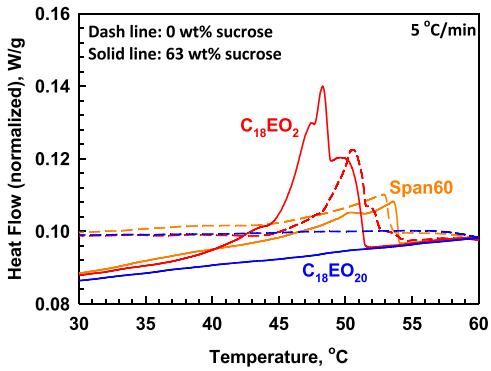

Fig. 2. DSC thermograms of aqueous solutions with 63 wt% sucrose (solid lines) and without sucrose (dashed lines) of Span60 (orange), $C_{18}EO_{20}$ (blue) and $C_{18}EO_2$ (red), measured at cooling rate of 5 °C/min. Surfactant level is 2 wt%.

The dispersions of oil-soluble surfactants show non-Newtonian response and their apparent viscosity decreases as a function of shear rate for both types of systems – with and without sucrose. As expected, the addition of sucrose strongly increases the viscosity of all solutions, see Fig. 3. It is seen from Fig. 3 that the apparent viscosities of $C_{18}EO_2$ and Span 60 solutions are very similar in presence of sucrose at high shear rates, relevant to foaming. To understand how the sucrose affects the interactions between the multi-lamellar vesicles formed in these dispersions, the relative viscosity (measured viscosity divided by the viscosity of the continuous phase) as a function of the shear rate is plotted in Fig. S2 in the Supporting information. These plots show that Span 60 increases to a larger extent the viscosity, as compared to $C_{18}EO_2$ for both types of solutions, with and without added sucrose. The relative effect of Span 60 aggregates is much more pronounced for the dispersions in deionized water, as compared to its effect for dispersions in sucrose solution.

From the experiments aimed to characterize the bulk properties (type of aggregates, thermal and rheological properties) of studied systems, one can conclude that the dispersions of oil-soluble surfactants contain multilamellar vesicles with melting temperature of ≈ 50 °C for

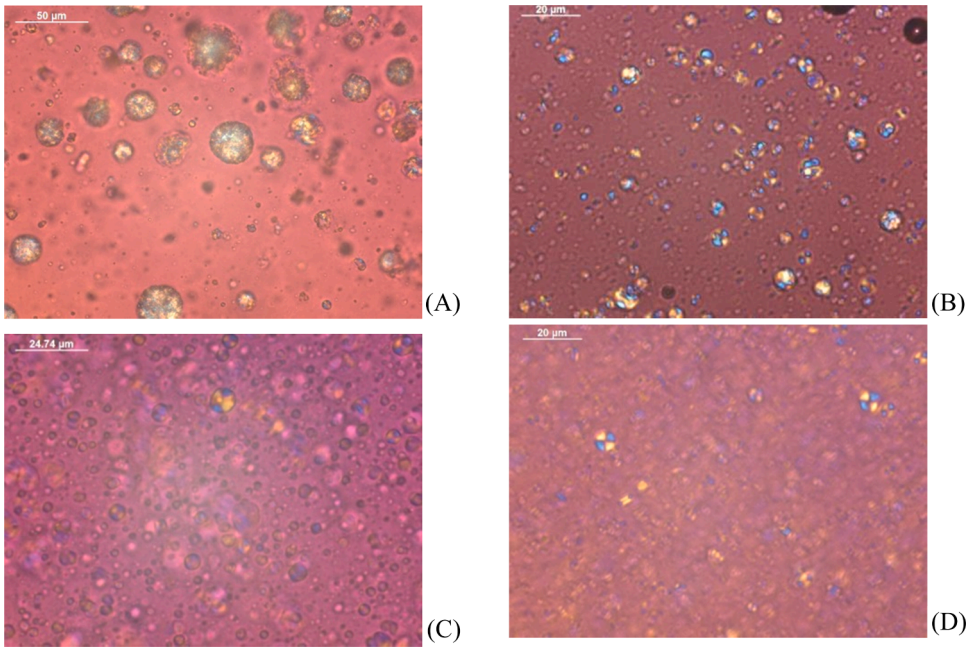

Fig. 1. Images in polarized light from solutions of (A, B) Span 60 and (C, D) $C_{18}EO_2$ in deionized water (A, C) or in 63 wt% sucrose solution (B, D). Surfactant level is 2 wt%.

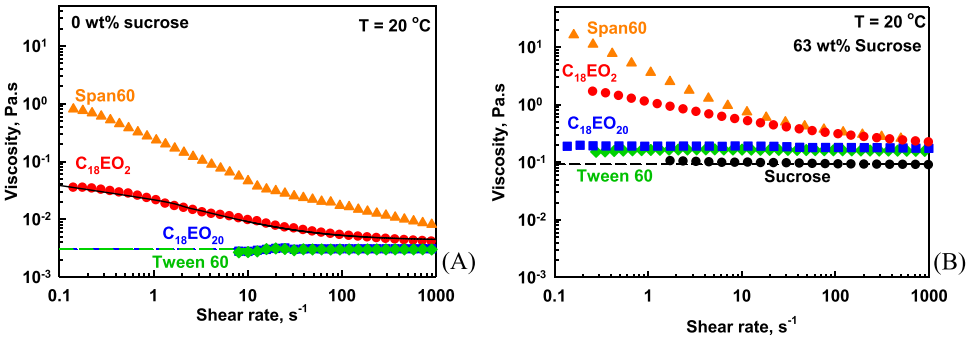

Fig. 3. Apparent viscosity as a function of shear rate for dispersions in (A) water and (B) 63 wt% sucrose. In both graphs the data for Span60 are shown with orange triangles, Tween 60 – green rhombus, $C_{18}EO_2$ – red circles, $C_{18}EO_{20}$ – blue squares. The viscosity of sucrose solutions without added surfactant is presented with black circles in (B). Continuous curves represent best fits to the experimental data for $C_{18}EO_2$ by Eq. (3). Surfactant level is 2 wt%.

$C_{18}EO_2$ and ≈ 53 °C for Span 60, whereas the micellar solutions are formed from water-soluble surfactants. The presence of multilamellar vesicles in dispersions of oil-soluble surfactants leads to non-Newtonian rheological response of them, whereas water-soluble solutions behave as Newtonian fluids with and without sucrose. The addition of sucrose to dispersions of oil-soluble surfactants increases significantly the enthalpy of phase transition for both oil soluble surfactants, which means that sucrose increases the ordering of molecules in MLV.

4. Surface properties

4.1. Surface tension isotherms

The surfactant solutions with different concentrations between 10^{-6} to 1 wt% were prepared by consecutive dilution of dispersions obtained by procedure described in Section 2.1. Upon dilution the dispersions of oil-soluble surfactants become less turbid, which is related to decrease number of MLV in the solutions. The solutions of water soluble surfactants are transparent under all dilutions. The prepared solutions are used for surface tension determination and typical curves from these measurements are shown in Fig. 4 for the highest surfactant concentration (2 wt%), which is used afterwards for foam generation. As can be seen from data presented in Fig. 4, the surface tension decreases with time and even after 900 s it does not reach its equilibrium value, which is related to slow adsorption of surfactant molecules on the solution surface from one side and to the fact that the used surfactants are wide mixture of different components, which leads to continuous change in the composition of the adsorption layer from other side. In order to determine how the concentration and the presence of sugar affect the surface properties the surface tension measured after 900 s of drop formation as a function of surfactant concentration is plotted in Fig. 5. The equilibrium surface tension cannot be determined for some of the solutions because there is a gradual decrease in the surface tension over time and it is not clear when the decrease will stop.

For water soluble surfactants the addition of sugar in the solution increases the surface tension at low surfactant concentrations and decreases it at high concentrations, whereas for oil-soluble surfactants the addition of sugar increases the surface tension in entire range of concentrations studied, see Fig. 5. The increased surface tension at low surfactant concentration for all studied surfactants is related to the fact that the surface tension of 63 wt% sucrose solution is higher by about 6 mN/m than that of deionized water, in agreement with the results reported in literature [47]. The increase of surface tension in presence of sugar for oil soluble surfactants at high concentration is in good agreement with optical observations and DSC measurements, that show that the addition of sugar increases the number of molecules that are well packed in MLV and as consequence the molecules prefer to stay in MLV instead going on the air-water interface. For water soluble surfactants again, the presence of sugar decreases the affinity of surfactant to adsorb on the air-water interface and as consequence the critical micellar concentration increases, but lower surface tension which is reached after CMC in sugar containing solutions when water soluble surfactants are used means that the sugar decreases the area per molecule in the equilibrium adsorption layer. Note that the surface pressure at CMC for $C_{18}EO_{20}$ dissolved in water is 31 mN/m, whereas for sugar containing solution is 42 mN/m. Assuming that Volmer equation describes the relation between surface pressure and surfactant adsorption and using the approach described in Ref. 11 and Eq. (5) therein one can calculate the surfactant adsorption at CMC for solution without sugar to be 3.1 μmol/m^2 and 3.3 μmol/m^2 in presence of sugar, respectively. This calculation shows that the area per molecule at CMC for Brij 58 decreases from 0.54 nm^2 to 0.50 nm^2 upon addition of sugar in the solution. Similar effect for decrease of surface tension was reported for $C_{12}EO_{10}$ surfactant upon addition of much lower sucrose concentration

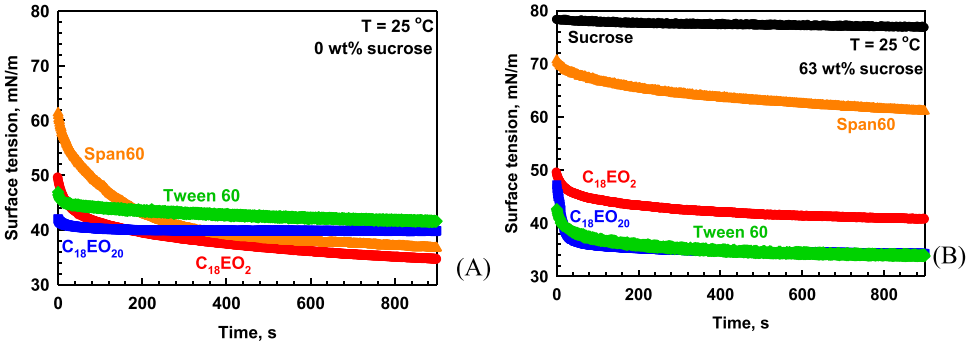

Fig. 4. Surface tension as a function of time (A) in the absence of sucrose and (B) in the presence of 63 wt% of sucrose, for 2 wt% surfactant solutions or dispersions: Span60 – orange triangles, Tween 60 – green rhombus, $C_{18}EO_2$ – red circles, $C_{18}EO_{20}$ – blue squares. Black circles in (B) present the data for sucrose solution without surfactant.

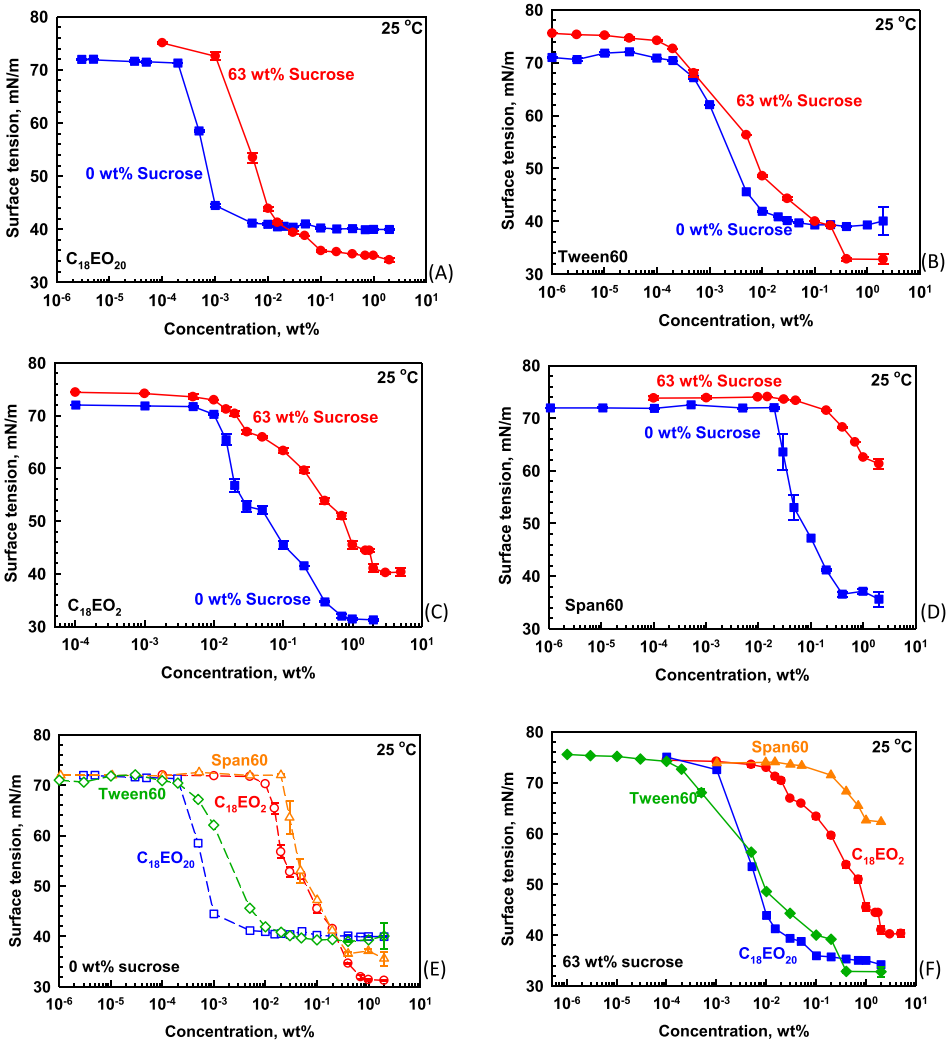

Fig. 5. Surface tension as measured by DSA apparatus after 900 s, as a function of surfactant concentration for (A) $C_{18}EO_{20}$; (B) Tween 60; (C) $C_{18}EO_2$; (D) Span 60 and comparison of the isotherms for solutions (E) without sugar and (F) in presence of 63 wt% sugar.

in Ref. [48].

The comparison of water-soluble and oil-soluble surfactants with and without added sugar in the solution is shown in Figs. 5F and 5E, respectively. It is seen that higher concentrations are needed for oil-soluble surfactants to start to decrease the surface tension and as a consequence the CMC for oil soluble surfactants is higher as compared to water soluble surfactants. The similar increase in critical micellar concentration with decrease the number of EO groups in $C_{16}EO_n$ surfactant series is shown in Ref. [49]. However, in most cases the opposite trend is reported in the literature for $C_{12}EO_n$ surfactants [50–52]. Most probably the difference is coming from the fact that $C_{12}EO_n$ surfactants at studied temperature formed lamellar phases of L_α, whereas longer-chain surfactants such as $C_{16}EO_n$ and $C_{18}EO_n$ formed lamellar phases of L_β at room temperature which strongly decreases the affinity of surfactant molecules to go on the air-water interface. After adsorbing on the air-water interface the surfactant with smaller number of EO groups in their head group show lower surface tension which is good agreement with results reported in the literature [49].

The addition of sucrose to the solutions increases significantly the following properties of oil soluble surfactants: CMC, surface tension below and above CMC, which means that the affinity of oil-soluble surfactants to go on air-water interface decreases with increasing the sugar concentration in the solution, which is related to better packing of the molecules in the MLV in the solution as can be seen from increased transition enthalpies shown in Table S1 in presence of sugar.

4.1.1. *Surface modulus measured with pendant drop method*

The surface moduli of the adsorption layers formed from 2 wt% solutions 10 min after forming the pendant drop by applying sinusoidal oscillations of the surface area at three periods of oscillation are measured and presented in Fig. S3 in the Supporting information.

The measured surface moduli for water-soluble surfactants in deionized water were much lower as compared to those for oil-soluble surfactants, as shown in Fig. 6A. This is due to the fast adsorption/desorption processes of the water-soluble surfactants. For oil-soluble surfactants, the rate of exchange between the bulk and surface is much slower and, hence, the measured surface moduli are higher. In addition, the oil-soluble surfactants pack more densely on the interface due to their smaller head-group and surface phase transition in the adsorption layer is expected to occur.

The addition of sucrose to the aqueous solutions increases the surface moduli for the water-soluble surfactants from 10 to 40 mN/m, indicating slower adsorption/desorption and formation of denser adsorption layers. On the other hand, the sucrose increases the surface moduli for $C_{18}EO_2$ and decreases significantly the surface moduli for Span 60, see Fig. 6. The later effect is related to the very low surface activity of Span 60 in the sucrose-containing solutions, cf. Fig. 4B above.

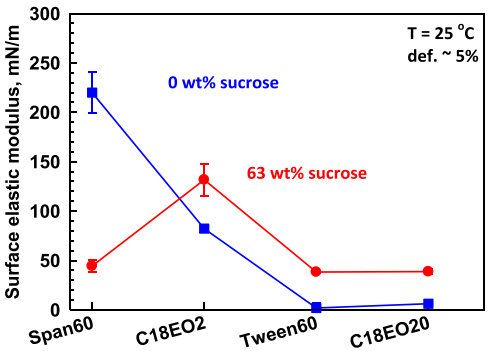

Fig. 6. Surface elastic moduli of the surfactant solutions in the absence (blue squares) and in the presence (red circles) of 63 wt% sucrose, as measured at 5% surface deformation and 5 s period of oscillations. Surfactant level is 2 wt%.

4.1.2. Surface modulus at slow deformations in Langmuir trough

In Langmuir trough the experiments started with measuring the equilibrium surface tension for 5 min. As in the case of pendant drop method, the surface tensions measured with oil-soluble surfactants in presence of sucrose were higher when compared to those in deionized water, whereas the opposite was observed for water-soluble surfactants.

The surface rheological properties of the adsorption layers were characterized under slow deformations (see Section 2.2.5), see Fig. 7. No change in the surface tension upon compression or expansion of the layer was observed for $C_{18}EO_{20}$ dissolved in water, see Fig. 7D, which means that this surfactant adsorbs/desorbs fast in the time-scale of the surface compression/expansion applied. In the presence of sucrose, no change in the surface tension upon compression was observed, while an increase in the surface tension by 2 mN/m was seen after starting the expansion. No further change in the surface tension was seen in the following period of expansion, see Fig. 7D.

The behavior of the adsorption layer of Tween 60 was slightly different. The surface tension decreased upon compression – an effect which was more pronounced in deionized water and, afterwards, increased upon expansion to reach the initial value. These changes in the surface tensions upon compressions and expansions were probably related to slow exchange of surfactant molecules between the solution and the interface. Note that the used Tween 60 contains surfactant molecules with long surfactant tails of C16 and C18 carbon atoms which probably exhibit a slow exchange during the experiments.

The behavior of adsorption layers formed from oil-soluble surfactants was qualitatively different. In all cases very fast decrease in the surface tension upon compression of the interface was observed, followed by plateau region in which the further decrease in the surface area did not change the surface tension. Upon expansion, again very fast initial increase of the surface tension was observed, which remained almost constant afterwards. This behavior could be explained with the formation of compact adsorption layer in the first stage of compression which did not change significantly afterwards, due to relaxation mechanisms from out-of-plane layer folding and/or forced desorption upon large compression. As it can be seen, more compact compressed layers with lower with ca. (9 mN/m of surface tension) were formed in the presence of sucrose even after starting at higher initial surface tension.

To compare the effect of compression and expansion on the surface tensions of the different solutions studied, the surface stress defined as the difference, $\Delta\sigma$, between the highest surface tension reached upon expansion and the lowest surface tension reached upon compression was determined, see Fig. 7C for illustration. The values of $\Delta\sigma$ for the various adsorption layers are compared in Fig. 8. One sees that the difference in the adsorption layers upon compression and expansion is much more pronounced for the oil-soluble surfactants as compared to the water-soluble ones. In addition, the presence of sucrose in the solution increases this difference for oil-soluble surfactants. The value of $\Delta\sigma \approx 46$ mN/m for Span 60 in the presence of sucrose is the highest in this series of experiments. In other words, the molecules of the hydrophobic surfactants pack very well during slow compression and form dense adsorption layers with surface tension as low as 10 mN/m. The presence of sucrose facilitates this compaction.

To determine how rapidly the compacted adsorption layers relax, the experiments in which the compacted layers were kept at constant

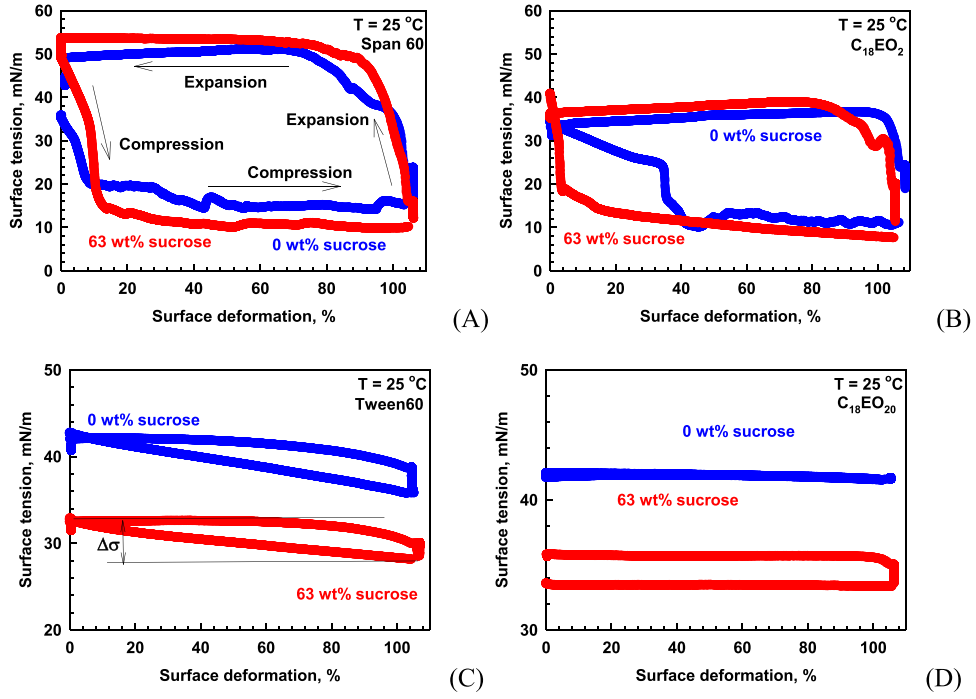

Fig. 7. Surface tension vs. surface deformation ($< 10^{-3}$ Hz) during compression and expansion of the surface layer formed from (A) Span 60, (B) $C_{18}EO_2$, (C) Tween 60, and (D) $C_{18}EO_{20}$ in the absence (blue circles) and in the presence (red circles) of sucrose. The experiments are performed in a Langmuir trough at 25 °C. Surfactant level is 2 wt%.

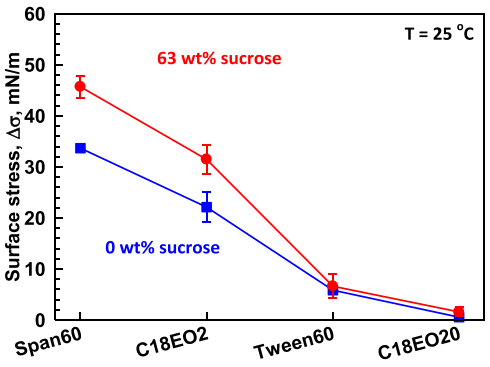

Fig. 8. Surface stress calculated as a difference between the maximal surface tension reached upon expansion and the minimal surface tension reached upon compression in the absence (blue squares) and in the presence (red circles) of sucrose. Surfactant level is 2 wt%.

surface area for 30 min and measured the rate of surface tension relaxation were performed. The results from these experiments are summarized in Fig. S4 in Supporting information. One sees that the surface tension for $C_{18}EO_{20}$ remains constant during compression and after stopping the compression when deionized water is used for solution preparation. On the other hand, slow increase in the surface tension after stopping the compression is observed when sucrose is present. Similar surface tension relaxation was observed for all other solutions studied. The surface tensions after compression and after relaxation (30 min after stopping the compression) are shown in Fig. 9. One sees that the surface tensions in presence of sucrose are lower after compression, as compared to those measured without sucrose. This trend is preserved even 30 min after the relaxation of compressed layers, see Fig. 9B, which means that sucrose always supports the formation of denser adsorption layers upon slow compression. Note that this is not true when the layers are formed without compression – in that case, the effect of sucrose is different for oil-soluble and water-soluble surfactants as seen in Fig. 4.

From all these series of experiments one can conclude that:

(1) The rate of surfactant exchange between bulk and interface is much slower when oil-soluble surfactants are used. As a consequence, the surface tension decreases slowly as compared to water-soluble surfactants as measured by pendant drop method. When measurements are performed in Langmuir trough under slow compression due to slow desorption of molecules from the interface the surface tension can reach value of ≈ 15 mN/m, whereas upon expansion the surface tension becomes of ≈ 50 mN/m, which leads to very big difference in the surface tension of compressed and expanded layers of ≈ 35 mN/m. The effect is even more pronounced in presence of sugar in the solution, where this difference becomes ≈ 45 mN/m.

(2) The faster exchange of surfactant molecules between the bulk and the interface for water-soluble surfactants leads to faster formation of dense adsorption layers for these surfactants, but upon slow compression and expansion of the layers the surface tension remains almost constant, which means that the bubbles in the foam will have similar surface tensions, which will facilitate the rate of Ostwald ripening. The addition of sucrose does not change the surface stress upon compression and expansion for these surfactants.

5. Foamability, foam stability and foam rheology

5.1. Foam volume and bubble size

The results about the rate of air entrapment (increase of foam volume or increase of overrun) in the various dispersions are compared in Fig. 10 and Fig. S5 in the Supporting information. As can be seen from presented data the overrun, Ψ, increases like exponent rise to maximum in the first 30 min and continue increasing for foams formed from solutions without added sugar or decreases for foams formed from sugar solutions in the next 30 min of mixing. The experimental data for overrun as a function of time for first 30 min of mixing are fitted by following equation:

$$\Psi = \Psi_{30}(1 - \exp(-t/t_{ch})) \quad (2)$$

Where Ψ is the overrun, Ψ_{30} is the maximal overrun reached in the first 30 min and t_{ch} is the characteristic time for foam generation. The obtained results for Ψ_{30}, t_{ch} and Ψ_{60} defined as overrun reached after 60 min of mixing are shown in Table 1. For foams prepared from solutions without sucrose the rate of foam generation is faster for water-soluble surfactants ($t_{ch} < 0.6$ min) and significantly slower for oil-soluble surfactants ($t_{ch} \geq 3$ min), which is in good agreement with slower decrease of surface tension for oil-soluble surfactants as shown in Fig. 4. In presence of sugar the rate of foam generation decreases (the characteristic time increases) for all studied surfactants except for $C_{18}EO_2$ for which it remains constant in the frame of our experimental accuracy.

The value of Ψ_{30} is lower as compared to Ψ_{60} for solutions without sugar, whereas the opposite trend is observed for sugar containing solutions. The value of overrun depends on the competition of two processes that occur simultaneously – air entrapment and coalescence of newly entrapped air with atmosphere [10]. The air entrapment depends on the ability of mixing device to entrap new air in the foam [35], whereas the coalescence depends on the ability of surfactants to stabilize the newly entrapped air [10]. For foams formed from solutions without sugar the rate of air entrapment is higher than the rate of coalescence of bubbles with atmosphere after 30 min of mixing, whereas the opposite trend is observed for sugar-containing foams. Most probably in both foams the process of coalescence between bubble and the atmosphere continues even after 30 min of mixing, however, for foams formed

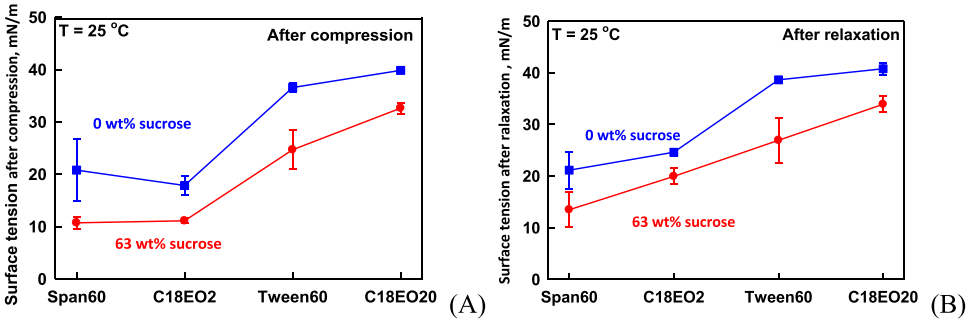

Fig. 9. (A) Surface tension after compression before starting the relaxation and (B) Surface tension after 30 min of relaxation after compression for adsorption layers of Span 60, Tween 60, $C_{18}EO_2$ and $C_{18}EO_{20}$ without sucrose (blue squares) and with added sucrose (red circles). Surfactant level is 2 wt%.

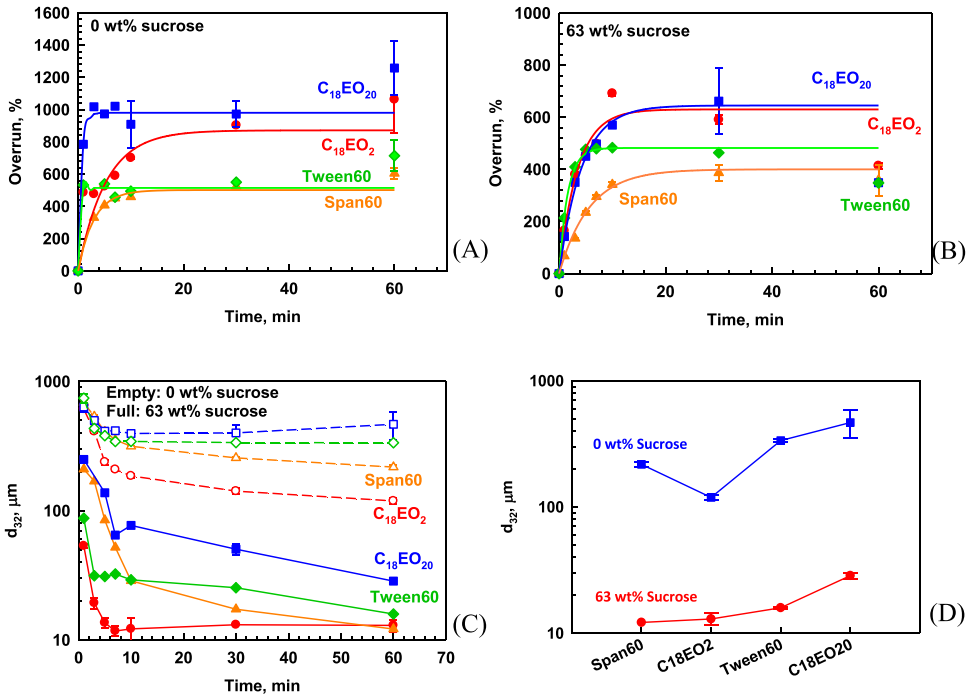

Fig. 10. (A, B) Overrun; (C, D) mean bubble size as a function of (A, C, D) aeration time and (D) used surfactant for dispersions with and without sucrose. Surfactant level is 2 wt%. The continuous curves in (A,B) are the best fit of experimental data obtained up to 30 min mixing with Eq. (2).

Table 1
The maximal overrun, Ψ_{30}, and characteristic time for foam generation, t_{ch}, as determined from the best fit of experimental data shown in Fig. 10 for first 30 min. The experimentally determined value for overrun measured 60 min after foam generation is also shown for comparison, Ψ_{60}.

Surfactant	No sugar			+ Sugar		
	t_{ch}, min	Ψ_{30}, %	Ψ_{60}, %	t_{ch}, min	Ψ_{30}, %	Ψ_{60}, %
Span 60	3 ± 0.3	500 ± 15	600 ± 40	5.6 ± 0.5	400 ± 15	360 ± 60
Tween 60	0.05	515 ± 20	700 ± 90	1.6 ± 0.1	480 ± 10	350 ± 40
$C_{18}EO_2$	5.3 ± 0.9	870 ± 60	1000 ± 200	4.5 ± 0.7	630 ± 40	410 ± 10
$C_{18}EO_{20}$	0.60 ± 0.09	980 ± 40	1250 ± 170	4.2 ± 0.3	650 ± 20	350 ± 40

without sugar the elasticity of the foams is relatively low and the mixing device can entrap further air in the foam. This effect compensates, in excess, the coalescence between bubbles and the atmosphere, which results in an increase of foam volume after 60 min in comparison to that measured after 30 min. In the case of sugar containing foams their elasticity increases significantly due to large decrease in bubble size and the higher initial viscosity. As a consequence, the mixing equipment cannot entrap further amount of air in the foam, resulting in a decrease of overrun upon further mixing from 30 to 60 min

The final overrun, Ψ_{60} is the same for water-soluble and oil-soluble surfactants having same type of surfactant head group, which means that the number of EO groups does not affect Ψ_{60}. Similar trend is observed for Ψ_{30} in presence of sugar. The addition of sugar decreases by $\approx$ 50% the maximal overrun which could be reached for all studied surfactants, which is related to higher viscosity of these solutions and lower bubble size for the sugar rich foams.

The bubble size in the foams after certain periods of foaming was also measured, see Fig. 10 C,D. It is seen that the mean bubble size decreases significantly with increasing the time of mixing in the first 10 min. Much slower decrease is observed at longer mixing times for foams formed from sucrose-containing dispersions, while no significant change in the bubble size is detected with water-soluble surfactants, in the absence of sucrose. The final bubble size in the foams formed without sucrose varied between 100 and 560 μm, whereas 10-times smaller bubbles were formed in the presence of sucrose – bubble size between 10 and 30 μm. Therefore, the presence of sucrose has huge effect on the bubble size in the foams formed. This very significant effect of sucrose on the bubble size is, at least partially, related to the increased viscosity of the dispersions in the presence of sugar [35]. Smaller in size bubbles are formed when oil-soluble surfactants are used. The latter effect is related to the higher surface moduli measured in these systems, in accordance with our previous studies [35,53].

After foam preparation the films that are formed between upper layer of bubbles and large interface were observed. The optical observations were performed in reflected light. The typical pictures from these observations are shown in Fig. 11. In these pictures the films appear dark when their thickness is below 20 nm, which is the case when $C_{18}EO_2$ and $C_{18}EO_{20}$ in water are used for foam preparation. The films are with thickness between 30 and 50 nm (appear gray) when the foams are stabilized by Tween 60 (with and without sugar) and $C_{18}EO_{20}$ (in presence of sugar). The thickness of the film is between 50 and 70 nm for foams stabilized by Span 60 (without sugar) and films with irregular thickness which means that MLV are entrapped in the films when oil-soluble surfactants in presence of sugar are used. These MLV can serve as reservoir for supply of surfactant molecules upon storage of formed foams.

5.1.1. *Foam stability*

In this section, the results about the stability of prepared foams upon storage at room temperature are presented. Illustrative pictures of the foams after 1 h, 1 day, 5 days and 10 days of storage are shown in Table 2, whereas the evolution of mean bubble size as a function of time

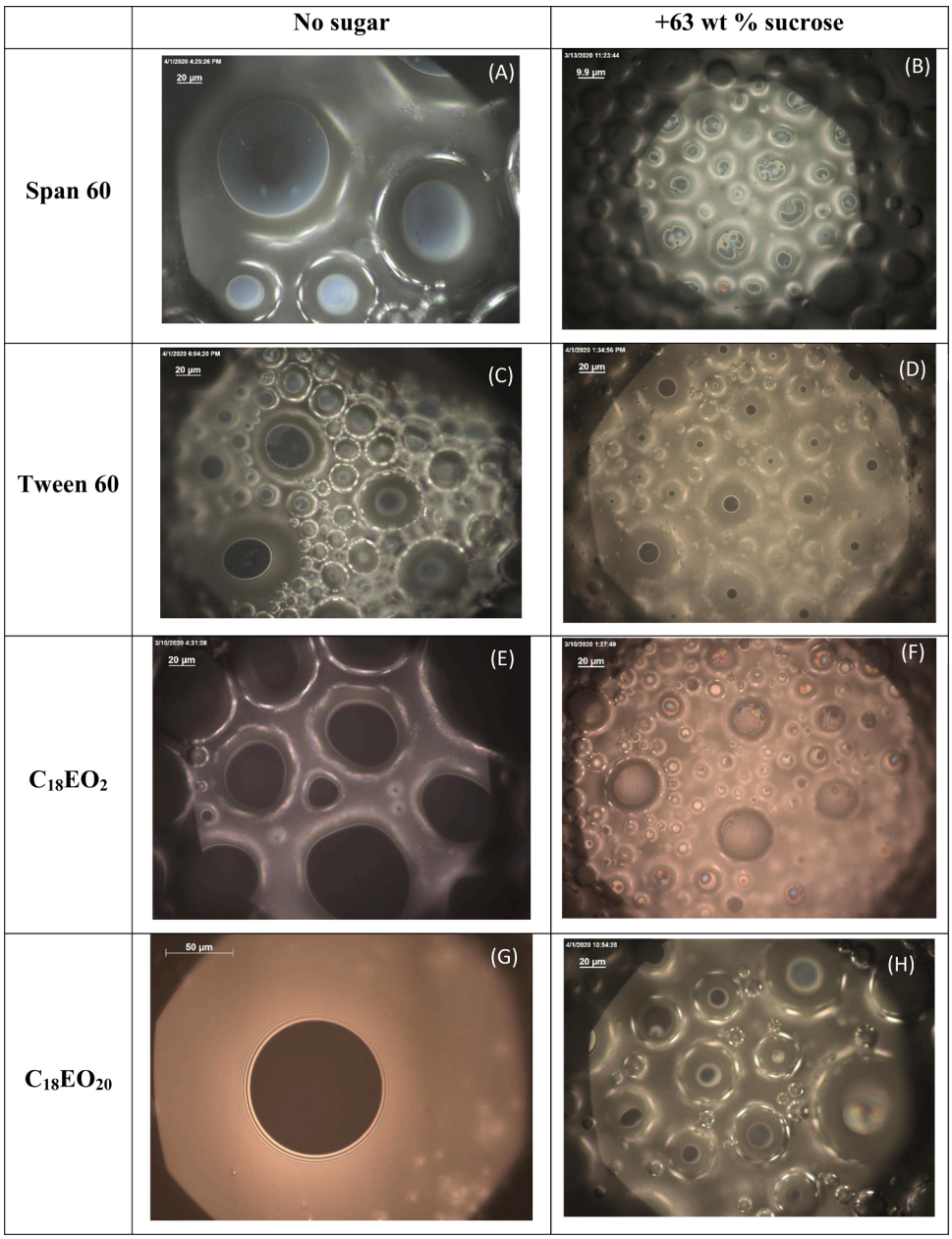

Fig. 11. Illustrative pictures of the film formed between upper layer of bubbles and atmosphere for foams stabilized by different surfactants in presence and absence of sucrose. The surfactant level is 2 wt%.

is shown in Fig. 12. One sees that all formed foams preserve their volume within 60 min after their formation. Part of the water drains during this period when water-soluble surfactant without sugar are used for foam stabilization. The mean bubble size increases very significantly during this period and bubbles with millimeter sizes are present after 60 min in these foams. The stability of all foams increases significantly when 63 wt % sugar is added in the aqueous phase. Part of this effect could be attributed to the lower gas solubility and the smaller diffusion coefficient of the gas molecules in sugar solutions, as compared to water [15]. However, again the foams formed with water-soluble surfactants are less stable as compared to the foams formed with oil-soluble surfactants. The lowest stability is measured with $C_{18}EO_{20}$, followed by Tween 60. In the foams prepared with $C_{18}EO_{20}$ significant fraction of centimeter sized bubbles are seen after 1 day of storage and part of the foam disappears. The water has drained at the bottom of the container for this sample. For Tween 60 foams, millimeter sized bubbles are observed on top of the foam and small fraction of the water is drained at the container bottom.

The visual appearance of the foams formed with oil-soluble surfactants in presence of sucrose is very similar after 1 day of storage – there is no water at the bottom and no big bubbles are seen in the foam. To check whether the size of the bubbles remains the same after 1 day of storage, the bubble size distribution was measured and compared to the initial bubble size distribution for these foams. It was found that the bubble size remained virtually the same when Span 60 was used, whereas a significant increase in the bubble size from 12 μm up to 80 μm was determined for $C_{18}EO_2$ stabilized foams.

As a rule, the rate of water drainage and the rate of bubble coalescence is slower for Tween 60 as compared to $C_{18}EO_{20}$ stabilized foams. The later effect is in good agreement with higher surface moduli and thicker films observed for Tween 60. After 1 day of storage these foams are destroyed completely due to Ostwald ripening and coalescence with atmosphere. The addition of sugar to water-soluble surfactants decreases the rate of water drainage and rate of Ostwald ripening as can be seen from presented pictures in Table 2 and again better stability is

Table 2
Pictures of the foams in glass containers after 60 min of foaming and after storage at 25 °C.

System	No Sugar				+Sugar			
	60 min	1 day	5 days	10 days	60 min	1 day	5 days	10 days
Span 60								
Tween 60								
$C_{18}EO_2$								
$C_{18}EO_{20}$		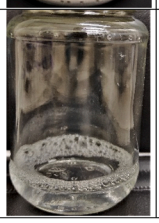	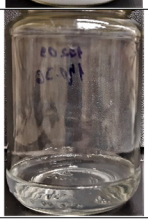					

25

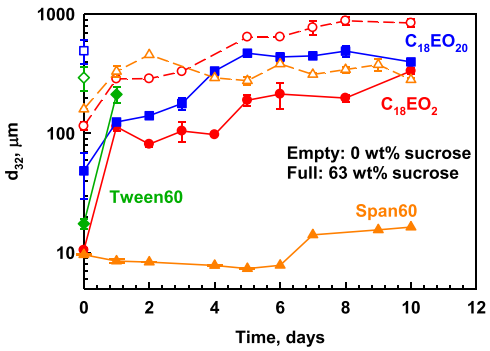

Fig. 12. Bubble size as a function of storage time for foams formed from different surfactant solutions. Foams stabilized by Tween 60 and $C_{18}EO_{20}$ solutions without sugar coalesce after 1 day of storage and that is why there is no data for them after that period.

determined for Tween 60 stabilized foams for which 1 day of storage leads to water drainage and significant increase in bubble size as can be seen from Fig. 12, but volume of the foam remains intact, whereas 50% of the initial foam disappears after 1 day when $C_{18}EO_{20}$ + sugar is used for its preparation. Foam half-life time for Tween 60 + sugar is ≈ 3 days.

The stability of foams containing oil-soluble surfactants is much better as compared to that of water-soluble surfactants with and without sugar. For foams stabilized by Span 60 (without sugar) the destabilization starts with water drainage and some increase in bubble size, whereas for $C_{18}EO_2$ stabilized foams first significant increase in the bubble size is observed and afterwards the water drainage takes place. When sugar is added to these solutions the foams formed by Span 60 + sugar remain visually stable for 10 days, whereas significant increase in bubble size is observed for foams stabilized by $C_{18}EO_2$ + sugar, see Fig. 12. The better stabilization of foams formed from oil-soluble surfactants is related to higher viscosity of the dispersion (see Fig. 3), but as can be seen from the results obtained with water-soluble surfactants in presence of sugar the increase of the viscosity is not enough to ensure good stabilization. The decreased rate of Ostwald ripening is related to much higher difference in the surface tension of shrinking and expanding bubbles which leads to lower driving force for gas transfer from smaller to bigger bubbles. Similar effects were reported for saponin stabilized foams where the difference in the surface tensions of expanding and shrinking bubbles lead to a significant deceleration of the bubble Ostwald ripening [16]. The good correlation between the measured surface stresses in the Langmuir trough and the foam stability upon storage (see Fig. 8 and Table 2) is seen. This difference is higher for Span 60 stabilized foams as compared to $C_{18}EO_2$ and as consequence the former foams are more stable.

5.1.2. Foam rheology

After preparing the foams we tried to determine their rheological response under oscillatory deformations and steady shear. The foams formed from water-soluble surfactants without sugar contained large bubbles and the water drained from these foams very quickly. After the initial fast water drainage, the Ostwald ripening accelerated and the bubbles increased their size even further, due to the increased air volume fraction and the increased area of the foam films between the neighboring bubbles. Therefore, we could not characterize the

rheological properties of these foams. The foam formed from Span 60 dispersion without sugar also suffered from fast water drainage and we could not characterize their rheological properties. The foams from $C_{18}EO_2$ dispersions remained stable and we were able to characterize their behavior with and without sucrose present. These are the results presented and discussed below.

The results from the amplitude sweep experiments, Fig. 13A, show that the foam formed from water dispersion has the typical "type III" response (G' decreases and G'' passes through a maximum as a function of the oscillation amplitude), whereas the foam formed from sucrose solutions has "type I" response with strain thinning [54]. It is known that type III behavior is typical for hard gels, laponite dispersions, and concentrated foams and emulsions [54–58]. Type I behavior is typical for melt gels and the origin of strain thinning is similar to the origin of shear thinning in the steady-shear experiments [54]. The difference in the rheological response of foams formed with and without sugar is caused by the different air volume fractions in these two foams (80% for sugar containing foam and 90% for foams without sugar). The lower air volume fraction in sugar containing foams is responsible for the strain thinning behavior, whereas the higher air volume fraction in sugar deprived foams leads to the type III behavior. Higher air volume fraction in foams without sugar leads to friction between the bubbles during oscillations, whereas the low air volume fraction in sugar containing foams leads to much smaller films between bubbles and main friction is in the continuous phase not between bubbles, which leads to their different rheological response.

At low values of the strain amplitude, γ_A, in the plateau region, both moduli do not change significantly with the increase of γ_A. Both the elastic and the viscous moduli are higher for sucrose containing foam when compared to those without sucrose. It is well known from the literature [59,60] that the elastic modulus depends on the surface tension and bubble size. To account for this effect, the data were replotted by scaling them with the values predicted by Princen & Kiss [59]:

$$G_P = 1.77\Phi^{1/3}\left(\Phi - \Phi_0\right)\frac{\sigma}{R_{32}};\ \Phi 0 = 0.72 \tag{3}$$

Where G_p is the modulus, Φ is the air volume fraction, σ is the surface tension, and R_{32} is the mean bubble radius. In this way, any deviation of the data from unity indicates atypical rheological behavior of the foam, due to other factors beside the equilibrium surface tension and bubble size. We tried to use for this analysis also the equation proposed by Mason et al. [60], but the obtained results were better described by Princen's equation, probably because the studied foams were polydisperse.

To scale the measured moduli a value for the surface tension of the bubbles is needed. As shown in Section 3, the surface tension measured with these systems depends strongly on the pre-history of the formed adsorption layers. For the system $C_{18}EO_2$ + sucrose, the surface tension of 41 mN/m with the pendant drop method is measured, while in the Langmuir trough, the value of ≈ 10 mN/m for compressed layer, and ≈ 20 mN/m for same compressed layer after relaxation of 30 min is measured. These three very different values of surface tension correspond to very different adsorption layers – spontaneously formed, highly compressed and relaxed after compression. In the foaming experiments, the bubble surfaces are exposed to multiple compressions and expansions during foaming and the adsorption layers are expected to be compressed on the bubble surfaces immediately after stopping the foam agitation. On the other hand, the adsorption layers have time to relax after foam generation and, therefore, we used the value of the surface tension after relaxation to scale the data by Eq. (3). The scaled foam moduli are shown as a function of the strain amplitude in Fig. 10B. One sees that after such scaling, the data for the storage modulus at small oscillations becomes very close to the moduli predicted by Princen & Kiss [59], for foam generated from water dispersion. In contrast, the scaled modulus for foams formed with sucrose is by 40% higher than the value predicted by Eq. (3). The latter results are related to the higher surface elasticity measured with $C_{18}EO_2$ layers in the presence of sucrose, see Fig. 6 above. Similar effect was observed previously for the rheological properties of saponin-stabilized emulsions with high surface elasticity [61].

Even after scaling, the loss modulus for foams prepared from sucrose containing dispersion is ≈ 4 times higher, as compared to the loss modulus of foam generated from water dispersion. This significant

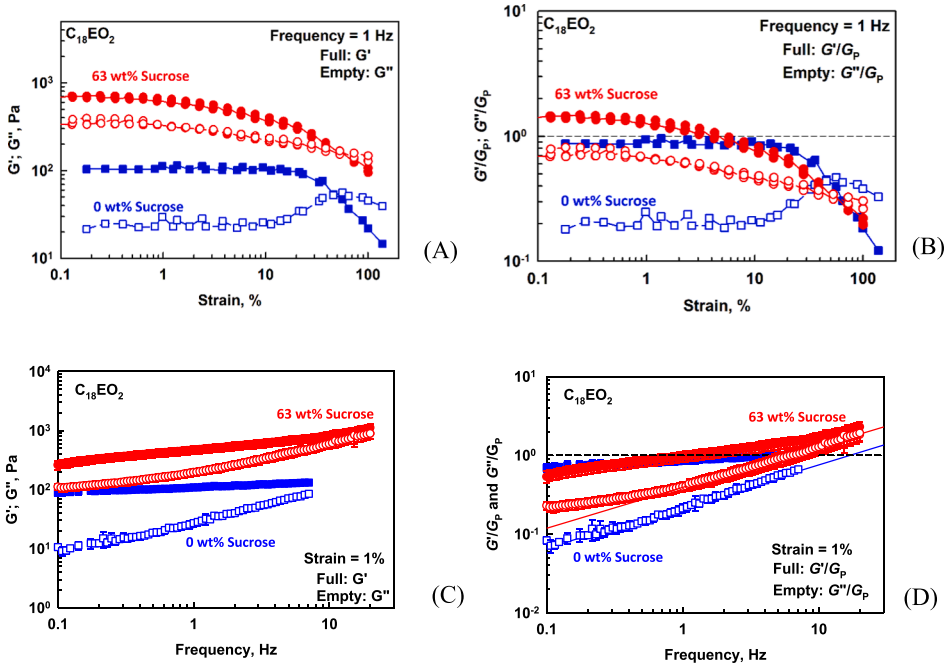

Fig. 13. Storage and scaled storage moduli (full symbols) and loss and scaled loss moduli (empty symbols) as functions of: (A, B) strain amplitude and (C, D) frequency of oscillation for foams prepared from $C_{18}EO_2$ dispersions in water (blue squares) or in sucrose solution (red circles). Surfactant level is 2 wt%. Strain amplitude, γ_A, is defined as maximal strain applied during oscillations at fixed frequency.

difference in the loss moduli is, at least partially, related to the higher viscosity of the continuous phase containing sugar which leads to higher dissipation of energy upon deformation. For both foams, the strain amplitude at which the viscous and loss moduli become equal is ≈ 50%.

The experimental results for the elastic and loss moduli as functions of oscillation frequency are shown in Fig. 13C. The scaled data are shown in Fig. 13D. It is seen that the elastic moduli for foams formed with and without sugar are very close to each other after scaling, but the loss moduli for foams prepared with sucrose remain higher, which means that the dissipation is more intensive in these foams. For both type of foams the determined values of $G'' \sim \omega^{0.5}$, which is in a good agreement with previous results reported in literature [62–66].

In the next series of experiments the rheological response of these foams upon steady shear deformation is described, see Fig. 14. The measured stress for sucrose-containing foams is much higher as compared to that for foams prepared with water dispersion. This difference is mainly due to the smaller bubble size and the higher viscosity of the continuous phase in the presence of sucrose.

From the best fit to the experimental data by the Herschel–Bulkley equation, the yield stress, τ_0, of the formed foams is determined, which is 43 Pa for foams formed in the presence of sucrose and 12 Pa for foams without sucrose. After accounting for the different bubble sizes and surface tensions, the dimensionless yield stress ($\tau_{DL} = \tau_0 R_{32}/\sigma_{relax}$) was 0.0158 for the sucrose-containing foam and 0.032 for the foam without sucrose. Note that the latter value is very close to the value of 0.033, predicted by Princen & Kiss [59]. This comparison shows that the higher yield stress of the sucrose containing foams is certainly related to the 10-times smaller bubbles in them, whereas the higher dimensionless yield stress for foams without sucrose is explained by the higher air volume fraction in them.

6. Main results and conclusions

The systematic series of experiments with two water-soluble (Brij S20 and Tween 60) and two oil-soluble (Brij72 and Span 60) surfactants are performed in the presence and in the absence of 63 wt% sucrose in the aqueous phase. The most important results are summarized below:

- The oil-soluble surfactants can be used for preparation of foams with very small bubbles. The formed foams show higher stability against water drainage, Ostwald ripening and coalescence as compared to the foams stabilized by water-soluble surfactants. The bubble size decreases and the foam stability is further enhanced when sugar is added into the surfactant solutions.
- The smaller bubbles in the foams formed from oil-soluble surfactants is related to the higher surface elasticity and the higher bulk viscosity of these solutions. The better stabilization against water drainage is related to the presence of multilamellar vesicles which increase the solution viscosity and to the viscoelastic adsorption layers formed with the oil-soluble surfactants. The slower rate of Ostwald ripening is explained with the large difference in the surface tension of the shrinking and expanding bubbles, which minimizes the driving force for gas transfer between the bubbles.
- The foams formed from 2 wt% Span 60 + 63 wt% sugar remain stable at 25 °C for more than 10 days, with bubble diameter below 10 μm.
- The rate of foaming is faster when water-soluble surfactants are used due to their fast adsorption on the bubble surface as compared to the oil-soluble surfactants. However, the formed foams contain larger bubbles and suffer from water drainage and bubble Ostwald ripening, due to the fast exchange of surfactant molecules between the bubble surface and the adjacent solution.
- The presence of sucrose strongly affects the foamability, foam stability and foam rheological properties for all systems studied. Foams containing 10 times smaller bubbles, with reduced air volume fraction (from 90% down to 80%), higher stability, higher storage and loss moduli, higher yield stress and higher viscous stress are formed in the presence of sucrose. The smaller bubbles and the lower air volume fraction in the presence of sucrose are explained by the higher viscosity of the foaming solutions.

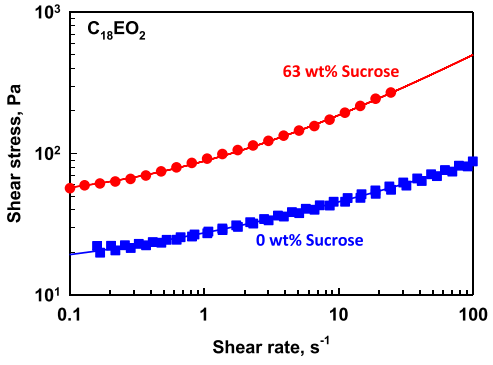

Fig. 14. Shear stress as a function of the shear rate for foams prepared from $C_{18}EO_2$ dispersions in water (blue squares) or in sucrose solution (red circles). Surfactant level is 2 wt%.

The overall conclusion from this work is that the oil-soluble surfactants can be used to prepare the foams with small bubbles which remain stable at room temperature for more than 10 days. So far in the literature it is known that the foams with such prolonged stability can be formed when hydrophobins [30,31], particles [16,17] or sucrose monostearin [28] are used. In the current study it was shown that oil soluble surfactants with 16 C-atom in their chain can be used as efficient foam stabilizer. This is attributed to their ability to decelerate the rate of Ostwald ripening by decreasing the driving force ensuring different surface tensions for shrinking and expanding bubbles and decreasing the permeability of gas molecules through the adsorption layer formed on bubble surfaces. In addition, it was shown that sugar can affect both the surface properties and the foam behavior and, therefore, it can be used as an active ingredient for modifying the properties of sweet foamy food products in a desired way.

The stable foams formed at high sugar concentration investigated in the current study can be transported at room temperature and diluted on site to obtain a confectionary product with desired sugar and bubble concentration. Possible directions for future work are (1) to compare the effect of hydrophobic chain length, hydrophilic head group and temperature on the foamability and stability of formed foams at high sugar concentration and (2) to determine the effect of sugar concentration on the properties of formed foams.

Funding

This work was partially supported by Unilever R&D Colworth, UK and by the Bulgarian Ministry of Education and Science under the National Research Programme "Healthy Foods for a Strong Bio-Economy and Quality of Life" approved by DCM #577/17.08.2018. F. Mustan is grateful to Operational program "Science and Education for Smart Growth", project BG05M2OP001–2.009–0028 for the financial support for scientific visit at Unilever R&D Colworth, UK.

CRediT authorship contribution statement

Fatmegyul Mustan: Investigation, Formal analysis, Visualization, Writing – original draft. **Nadya Politova:** Methodology. **Damiano Rossetti:** Conceptualization, Methodology, Funding acquisition. **Pip Rayment:** Conceptualization, Methodology, Funding acquisition. **Slavka Tcholakova:** Conceptualization, Methodology, Formal analysis, Writing – review & editing, Supervision, Funding acquisition.

Declaration of Competing Interest

The authors declare that they have no known competing financial interests or personal relationships that could have appeared to influence the work reported in this paper.

Acknowledgements

We are grateful to Prof. Nikolai Denkov (Sofia University) for the insightful discussions and for the critical reading of the manuscript.

Conflict of interest

None.

Associated content

*S Supporting Information.

Appendix A. Supporting information

Supplementary data associated with this article can be found in the online version at doi:10.1016/j.colsurfa.2021.127874.

References

[1] S. Lee, J. Lee, H. Yu, J. Lim, Synthesis of environment friendly nonionic surfactants from sugar base and characterization of interfacial properties for detergent application, J. Ind. Eng. Chem. 38 (2016) 157–166, https://doi.org/10.1016/j.jiec.2016.04.019.

[2] J. Jiao, Polyoxyethylated nonionic surfactants and their applications in topical ocular drug delivery, Adv. Drug Deliv. Rev. 60 (2008) 1663–1673, https://doi.org/10.1016/j.addr.2008.09.002.

[3] D.G. Sullivan, R.C. Nuti, C.C. Truman, Evaluating a nonionic surfactant as a tool to improve water availability in irrigated cotton, Hydrol. Process. 23 (2009) 2326–2334, https://doi.org/10.1002/hyp.7330.

[4] X. Wang, J.-M. Ruan, Q.-Y. Chen, Effects of surfactants on the microstructure of porous ceramic scaffolds fabricated by foaming for bone tissue engineering, Mater. Res. Bull. 44 (2009) 1275–1279, https://doi.org/10.1016/j.materresbull.2009.01.004.

[5] S.V. Ravikumar, J.M. Jha, S.S. Mohapatra, S.K. Pal, S. Chakraborty, Experimental investigation of effect of different types of surfactants and jet height on cooling of a hot steel plate, J. Heat. Transf. 136 (2014), 072102, https://doi.org/10.1115/1.4027182.

[6] R. Zolfaghari, A. Fakhru'l-Razi, L.C. Abdullah, S.S.E.H. Elnashaie, A. Pendashteh, Demulsification techniques of water-in-oil and oil-in-water emulsions in petroleum industry, Sep. Purif. Technol. 170 (2016) 377–407, https://doi.org/10.1115/1.4027182.10.1016/j.seppur.2016.06.026.

[7] Z.-L. Chen, Y.-L. Yan, X.-B. Huang, Stabilization of foams solely with polyoxyethylene-type nonionic surfactant, Colloids Surf. A: Physicochem. Eng. Asp. 331 (2008) 239–244, https://doi.org/10.1016/j.colsurfa.2008.08.011.

[8] X.-T. Li, Z.-L. Wu, Y.-L. Zhao, Y.-M. Wu, Understanding of the foam capability of sugar-based nonionic surfactant from molecular level, Colloids Surf. A: Physicochem. Eng. Asp. 551 (2018) 165–173, https://doi.org/10.1016/j.colsurfa.2018.05.010.

[9] M.D. Eisner, S.A.K. Jeelani, L. Bernhard, E.J. Windhab, Stability of foams containing proteins, fat particles and nonionic surfactants, Chem. Eng. Sci. 62 (2007) 1974–1987, https://doi.org/10.1016/j.ces.2006.12.056.

[10] B. Petkova, S. Tcholakova, M. Chenkova, K. Golemanov, D. Thorley, S. Stoyanov, Foamability of aqueous solutions: Role of surfactant type and concentration, Adv. Colloid Interface Sci. 276 (2020), 102084, https://doi.org/10.1016/j.cis.2019.102084.

[11] B. Petkova, S. Tcholakova, N. Denkov, Foamability of surfactant solutions: Interplay between adsorption and hydrodynamic conditions, Colloids Surf. A: Physicochem. Eng. Asp. 626 (2021), 127009, https://doi.org/10.1016/j.colsurfa.2021.127009.

[12] F.O. Opawale, D.J. Burgess, Influence of interfacial properties of lipophilic surfactants on water- in-oil emulsion stability, J. Colloid Interface Sci. 197 (1998) 142–150, https://doi.org/10.1006/jcis.1997.5222.

[13] Y. Fan, S. Simon, J. Sjöblom, Chemical destabilization of crude oil emulsions: Effect of nonionic surfactants as emulsion inhibitors, Energy Fuels 23 (2009) 4575–4583, https://doi.org/10.1021/ef900355d.

Z. Mitrinova, S. Tcholakova, J. Popova, N. Denkov, B. Dasgupta, K. P. Ananthapadmanabhan, Efficient control of the rheological and surface properties of surfactant solutions containing C8−C18 fatty acids as cosurfactants, Langmuir 29 (2013) 8255–8265, https://doi.org/10.1021/la401291a.

[15] S. Tcholakova, Z. Mitrinova, K. Golemanov, N.D. Denkov, M. Vethamuthu, K. P. Ananthapadmanabhan, Control of ostwald ripening by using surfactants with high surface modulUs, Langmuir 27 (2011) 14807–14819, https://doi.org/10.1021/la203952p.

[16] S. Tcholakova, F. Mustan, N. Pagureva, K. Golemanov, N.D. Denkov, E.G. Pelan, S. D. Stoyanov, Role of surface properties for the kinetics of bubble ostwald ripening in saponin-stabilized foams, Colloids Surf. A 534 (2017) (2017) 16–25, https://doi.org/10.1016/j.colsurfa.2017.04.055.

[17] I. Lesov, S. Tcholakova, M. Kovadjieva, T. Saison, M. Lamblet, N. Denkov, Role of pickering stabilization and bulk gelation for the preparation and properties of solid silica foams, J. Colloid Interface Sci. 504 (2017) 48–57, https://doi.org/10.1016/j.jcis.2017.05.036.

[18] L.J. Peltonen, J. Yliruusi, Surface pressure, hysteresis, interfacial tension, and CMC of four sorbitan monoesters at water–air, water–hexane, and hexane–air interfaces, J. Colloid Interface Sci. 227 (2000) 1–6, https://doi.org/10.1006/jcis.2000.6810.

[19] S. Demand, EggerS, P. Degen, P. Salmen, M. Paulus, M. Tolan, H. Rehage, New approach to structure–property correlations of different films of sorbitan esters and their self-assembly into viscoelastic monolayers, J. Surfact Deterg. 22 (3) (2019) 597–611, https://doi.org/10.1002/jsde.12261.

[20] Md.N. Islam, T. Kato, Influence of temperature and headgroup size on condensed-phase patterns in Langmuir monolayers of some oxyethylenated nonionic surfactants, Langmuir 21 (6) (2005) 2419–2424, https://doi.org/10.1021/la047544p.

[21] Md.N. Islam, T. Kato, Influence of temperature and alkyl chain length on phase behavior in Langmuir monolayers of some oxyethylenated nonionic surfactants, J. Colloid Interface Sci. 294 (2) (2006) 288–294, https://doi.org/10.1016/j.jcis.2005.07.023.

[22] K.R. Goldfein, J.L. Slavin, Why Sugar Is Added to Food: Food Science 101, Compr. Rev. Food Sci. Food Saf. 14 (2015) 644–656, https://doi.org/10.1111/1541-4337.12151.

[23] I.C.O. Neves, J.T. Faria, M.C.T.R. Vidigal, P.C. Fidelis, V.P.R. Minim, L.A. Minim, Foaming properties of suspensions composed by β-lactoglobulin and polysaccharides, in the presence of sucrose or polyols, Colloids Surf. A 550 (2018) 199–208, https://doi.org/10.1016/j.colsurfa.2018.04.039.

[24] J.R. Clarkson, Z.F. Cui, R.C. Darton, Effect of solution conditions on protein damage in foam, Biochem. Eng. J. 4 (2000) 107–114, https://doi.org/10.1016/S1369-703X(99)00038-8.

[25] M.S. Sadahira, M.I. Rodrigues, M. Akhtar, B.S. Murray, F.M. Netto, Influence of pH on foaming and rheological properties of aerated high sugar system with egg white protein and hydroxypropylmethylcellulose, LWT - Food Sci. Technol. 89 (2018) 350–357, https://doi.org/10.1016/j.lwt.2017.10.058.

[26] K. Lau, E. Dickinson, Structural and rheological properties of aerated high sugar systems containing egg albumen, JFS: Food Eng. Phys. Prop. 69 (2004) 5, https://doi.org/10.1111/j.1365-2621.2004.tb10714.x.

[27] K. Lau, E. Dickinson, Instability and structural change in an aerated system containing egg albumen and invert sugar, Food Hydrocoll. 19 (2005) 111–121, https://doi.org/10.1016/j.foodhyd.2004.04.020.

[28] E. Dressaire, R. Bee, D.C. Bell, A. Lips, H.A. Stone, Interfacial polygonal nanopatterning of stable microbubbles, Science 320 (2008) 1198–1201, https://doi.org/10.1126/science.1154601.

[29] P.J. Beltramo, M. Gupta, A. Alicke, I. Liascukiene, D.Z. Gunes, C.N. Baroud, J. Vermant, Arresting dissolution by interfacial rheology design, PNAS 114 (2017) 10373–10378, https://doi.org/10.1073/pnas.1705181114.

[30] A.R. Cox, D.L. Aldred, A.B. Russell, Exceptional stability of food foams using class II hydrophobin HFBII (Pages), Food Hydrocoll. Volume 23 (Issue 2) (2009) 366–376, https://doi.org/10.1016/j.foodhyd.2008.03.001.

[31] L.M. Dimitrova, P.V. Petkov, P.A. Kralchevsky, S.D. Stoyanov, E.G. Pelan, Production and characterization of stable foams with fine bubbles from solutions of hydrophobin HFBII and its mixtures with other proteins, ISSN 0927-7757, Colloids Surf. A: Physicochem. Eng. Asp. Volume 521 (2017) 92–104, https://doi.org/10.1016/j.colsurfa.2016.06.018.

[32] L. Ma, Q. Li, Z. Du, E. Su, X. Liu, Z. Wan, X. Yang, A natural supramolecular saponin hydrogelator for creation of ultrastable and thermostimulable food-grade foams, Adv. Mater. Interfaces 6 (2019), 1900417, https://doi.org/10.1002/admi.201900417.

[33] A.-L. Fameau, A. Saint-Jalmes, F. Cousin, B. HouinsouHoussou, B. Novales, L. Navailles, F. Nallet, C. Gaillard, F. Boué, J.-P. Douliez, Smart Foams: Switching Reversibly between Ultrastable and Unstable Foams, 11826-11826, Angew. Chem. Int. Ed. 50 (2011) 8264–8269, https://doi.org/10.1002/anie.201102115.

[34] T.D. Gurkov, J.T. Petkov, B. Campbell, R.P. Borwankar, Dilatational and Shear Rheology of Protein Layers on Water/Air Interface, in: E. Dickinson, R. Miller (Eds.), "Food Colloids, Fundamentals of Formulation", Royal Soc. Chem., Cambridge, UK, 2001, pp. 181–190.

[35] N. Politova, S. Tcholakova, Z. Valkova, K. Golemanov, N.D. Denkov, Self-regulation of foam volume and bubble size during foaming via shear mixing, Colloids Surf. A 539 (2018) 18–28, https://doi.org/10.1016/j.colsurfa.2017.12.006.

[36] Garrett, P.R., Hines, J.D., Joyce, S.C., & Whittal, P.T. (1993). Report prepared for Unilever R&D, Port Sunlight.

[37] D.J. Mitchell, G.J.T. Tiddy, L. Waring, T. Bostock, M.P. McDonald, Phase behaviour of polyoxyethylene surfactants with water. Mesophase structures and partial miscibility (cloud points), J. Chem. Soc., Faraday Trans. 1: Phys. Chem. Condens. Phases 79 (4) (1983) 975–1000.

[38] P. Mukherjee, S.K. Padhan, S. Dash, S. Patel, B.K. Mishra, Clouding behaviour in surfactant systems, Adv. Colloid Interface Sci. 162 (2011) 59–79, https://doi.org/10.1016/j.cis.2010.12.005.

[39] R.I. Strey, Experimental facts water-nonionic surfactant systems, the of effect of additives, Phys. Chem. Chem. Phys. 100 (1996) 182–189, https://doi.org/10.1002/bbpc.19961000303.
[40] T. Inoue, H. Ohmura, D. Murata, Cloud point temperature of polyoxyethylene-type nonionic surfactants and their mixtures, J. Colloid Interface Sci. 258 (2003) 374–382, https://doi.org/10.1016/S0021-9797(02)00162-5.
[41] M. Redkar, P.A. Hassan, V. Aswal, P. Devarajan, Onion Phases of PEG-8 Distearate, J. Pharm. Sci. 96 (2007) 2436–2445, https://doi.org/10.1002/jps.20863.
[42] Stefan Müller, Claus Börschig, Wolfram Gronski, Claudia Schmidt, Didier Roux, Shear-induced states of orientation of the lamellar phase of C12E4/Water, Langmuir 15 (22) (1999) 7558–7564, https://doi.org/10.1021/la9904105.
[43] F. Caboi, M. Monduzzi, Didodecyldimethylammonium bromide vesicles and lamellar liquid crystals. a multinuclear NMR and optical microscopy study, Langmuir 12 (15) (1996) 3548–3556, https://doi.org/10.1021/la951057f.
[44] N. Jibry, R.K. Heenan, S. Murdan, Amphiphilogels for drug delivery: formulation and characterization, Pharm. Res. 21 (2004) 1852–1861, https://doi.org/10.1023/B:PHAM.0000045239.22049.70.
[45] I. Heertje, E.C. Roijers, H.A.C.M. Hendrickx, Liquid Crystalline Phases in the Structuring of Food Products, Lebensm. -Wiss. U. -Technol. 31 (1998) 387–396, https://doi.org/10.1006/fstl.1998.0369.
[46] N. Duerr-Auster, J. Kohlbrecher, T. Zuercher, R. Gunde, P. Fischer, E. Windhab, Microstructure and stability of a lamellar liquid crystalline and gel phase formed by a polyglycerol ester mixture in dilute aqueous solution, Langmuir 23 (26) (2007) 12827–12834, https://doi.org/10.1021/la702242v.
[47] M.K. Supran, J.C. Acton, A.J. Howell, R.L. Saffle, Surface tension of common aqueous and organic phases in food emulsions, J. Milk. Food Technol. 34 (1971) 584–585.
[48] S.B. Sulthana, S.G.T. Bhat, A.K. Rakshit, Studies of the effect of additives on the surface and thermodynamic properties of poly(oxyethylene(10)) lauryl ether in aqueous solution, Langmuir 13 (1997) 4562–4568, https://doi.org/10.1021/la960527i.
[49] Z. Zhang, G. Xu, F. Wang, G. Du, Aggregation behaviors and interfacial properties of oxyethylated nonionic surfactants, J. Dispers. Sci. Technol. 26 (2005) 297–302, https://doi.org/10.1081/DIS-200049580.
[50] P.X. Li, Z.X. Li, H.-H. Shen, R.K. Thomas, J. Penfold, J.R. Lu, Application of the Gibbs equation to the adsorption of nonionic surfactants and polymers at the air-water interface: Comparison with surface excesses determined directly using neutron reflectivity, Langmuir 29 (2013) 9324–9334, https://doi.org/10.1021/la4018344.
[51] J. Lucassen, D. Giles, Dynamic surface properties of nonionic surfactant solutions, J. Chem. Soc., Faraday Trans. 1: Phys. Chem. Condens. Phases 71 (1975) 217–232, https://doi.org/10.1039/F19757100217.
[52] J. Penfold, R.K. Thomas, P.X. Li, J.T. Petkov, I. Tucker, J.R.P. Webster, A.E. Terry, Adsorption at Air-Water and Oil-Water Interfaces and Self-Assembly in Aqueous Solution of Ethoxylated Polysorbate Nonionic Surfactants, Langmuir 31 (2015) 3003–3011, https://doi.org/10.1021/acs.langmuir.5b00151.
[53] K. Golemanov, S. Tcholakova, N.D. Denkov, K.P. Ananthapadmanabhan, A. Lips, Breakup of Bubbles and Drops in Steadily Sheared Foams and Concentrated Emulsions, Phys. Rev. E 78 (2008), 051405, https://doi.org/10.1103/PhysRevE.78.051405.
[54] K. Hyun, S.H. Kim, K.H. Ahn, S.J. Lee, Large amplitude oscillatory shear as a way to classify the complex fluids, J. Non-Newton. Fluid Mech. 107 (2002) 51–65, https://doi.org/10.1016/S0377-0257(02)00141-6.
[55] X. Li, E.-K. Park, K. Hyun, Rheological analysis of core-stabilized Pluronic F127 by semi-interpenetrating network (sIPN) in aqueous solution, J. Rheol. 62 (2018) 107–120, https://doi.org/10.1122/1.5009202.
[56] X. Li, K. Hyun, Rheological study of the effect of polyethylene oxide (PEO) homopolymer on the gelation of PEO-PPO-PEO triblock copolymer in aqueous solution, Korea-Aust. Rheol. J. 30 (2018) 109–125, https://doi.org/10.1007/s13367-018-0012-z.
[57] V. Carrier, G. Petekidisa, Nonlinear rheology of colloidal glasses of soft thermosensitive microgel particles, J. Rheol. 53 (2009) 245–274, https://doi.org/10.1122/1.3045803.
[58] F. Rouyer, S. Cohen-Addad, R. Hohler, P. Sollich, S.M. Fielding, The large amplitude oscillatory strain response of aqueous foam: Strain localization and full stress Fourier spectrum, Eur. Phys. J. E 27 (2008) 309–321, https://doi.org/10.1140/epje/i2008-10382-7.
[59] H.M. Princen, A.D. Kiss, Rheology of foams and highly concentrated emulsions III, Satic Shear Modul. J. Colloid Interface Sci. 112 (1986) 427–437, https://doi.org/10.1016/0021-9797(86)90111-6.
[60] T.G. Mason, J. Bibette, D.A. Weitz, Yielding and flow of monodisperse emulsions, J. Colloid Interface Sci. 179 (1996) 439–448, https://doi.org/10.1006/jcis.1996.0235.
[61] S. Tsibranska, S. Tcholakova, K. Golemanov, N. Denkov, E. Pelan, S.D. Stoyanov, Role of interfacial elasticity for the rheological properties of saponin-stabilized emulsions, J. Colloid Interface Sci. 564 (2020) 264–275, https://doi.org/10.1016/j.jcis.2019.12.108.
[62] R. Hohler, S. Cohen-Addad, Rheology of liquid foam, J. Phys.: Condens. Matter 17 (2005) R1041–R1069, https://doi.org/10.1088/0953-8984/17/41/R01.
[63] N.D. Denkov, S. Tcholakova, K. Golemanov, K.P. Ananthpadmanabhan, A. Lips, The role of surfactant type and bubble surface mobility in foam rheology, Soft Matter 5 (2009) 3389–3408, https://doi.org/10.1039/B903586A.
[64] A. Bussonnière, I. Cantat, Local origin of the visco-elasticity of a millimetric elementary foam, J. Fluid Mech. 922 (2021) A25, https://doi.org/10.1017/jfm.2021.529.
[65] K. Krishan, A. Helal, R. Höhler, S. Cohen-Addad, Fast relaxations in foam, Phys. Rev. E 82 (2010), 011405, https://doi.org/10.1103/PhysRevE.82.011405.
[66] A.D. Gopal, D.J. Durian, Relaxing in foam, Phys. Rev. Lett. 91 (2003) 18, https://doi.org/10.1103/PhysRevLett.91.188303.